https://doi.org/10.5194/egusphere-2026-3829
Preprint. Discussion started: 25 August 2026

Interaction between magnetic topology and plasma dynamics in the quasi-steady solar wind-magnetosphere system under obliquely northward IMF conditions
- Basic idea and magnetic field structure of the system -

Shigeru Fujita[1], Masakazu Watanabe[2,3], Takashi Tanaka[3], Dong Sheng Cai[4]

[1]Center for Data Assimilation Research and Applications, The Institute of Statistical Mathematics, Research Organization of Information and Systems, Tachikawa, 190-0014, Japan
[2]Department of Earth and Planetary Sciences, Faculty of Science, Kyushu University, Fukuoka 819-0395, Japan
[3]International Research Center for Space and Planetary Environmental Science, Kyushu University, Fukuoka 819-0395, Japan
[4]Nagoya University of Merchandise and Business, Nisshin, Aichi 470-0193, Japan

Correspondence to: Shigeru Fujita (sfujita@ism.ac.jp)

Abstract. Conventional explanations for the formation of the solar wind–magnetosphere structure assume that the magnetic-field configuration is determined primarily by force balance and that reconnection subsequently occurs within the local topology formed by the IMF and the magnetospheric magnetic field. By contrast, because the vacuum magnetic field provides the background topology for global reconnection, force balance and the topology of the vacuum magnetic field should be regarded as playing equally important roles in determining the solar wind–magnetosphere structure. To elucidate how magnetic topology influences magnetic-field deformation and the resulting plasma dynamics, we investigate global magnetohydrodynamic (MHD) simulations that describe the behavior of a supersonic plasma flow in a background vacuum magnetic field characterized by the topology. In particular, we re-examine the MHD process from the perspective of the interaction between plasma dynamics and the deformation of the background magnetic field, and reinterpret the simulation results in the obliquely northward IMF conditions accordingly. It should be noted that the vacuum magnetic field represents the lowest magnetic-energy state. During the interaction, the force exerted by the plasma on the magnetic field is balanced by the opposing Lorentz force of the deformed magnetic field. The Lorentz force consists of the restoring force associated with deformation of the vacuum magnetic field and the magnetic pressure exerted by the magnetic flux transported into the magnetosphere through global magnetic reconnection. This force balance is referred to as the *mechanical principle*. Furthermore, because the two-null, two-separator structure is generally conserved and the positions of the null points remain nearly fixed in the obliquely northward IMF conditions, the magnetic field deforms subject to this topological constraint. This property is referred to as the *topology-conservation property*. This paper focuses on the global magnetic-field structure of the solar wind–magnetosphere system governed by these two fundamental physical laws. The main results are as follows. (1) The open magnetotail field lines that

https://doi.org/10.5194/egusphere-2026-3829
Preprint. Discussion started: 25 August 2026

extend from a null point toward the nightside are stretched antisunward by the solar-wind flow in the near-Earth region, whereas in the distant magnetotail they gradually bend toward the IMF direction owing to the restoring force associated with the vacuum magnetic field. (2) The open field lines that extend from one null point toward the dayside separator and pass through the other null point remain directly connected to the IMF owing to the topology conservation property. Consequently, the dayside part of the cylinder undergoes little deformation, thereby causing the cylinder opening to become highly elongated and form a narrow slit-like structure. (3) The nightside separator is stretched in the antisunward direction because the two cylinders formed by the open field lines deform so as to overlap. This deformation indicates that the closed-field-line region extends into the magnetotail. Thus, the plasma sheet is formed.

1 Introduction

1.1 Motivation of this study

In a steady state, the magnetic field and plasma in both the solar wind and the magnetosphere dynamically interact across the magnetopause to form the large-scale structure of the solar wind–magnetosphere system. By this dynamical interaction, compression of the magnetosphere by the solar wind plasma dynamic pressure induces the magnetopause current, which strengthens the magnetic field in the dayside magnetosphere and stretches the nightside magnetosphere into a long magnetotail [Nishida, 1978; Hughes, 1995; Russell et al., 2016]. In addition, magnetic reconnection between the interplanetary magnetic field (IMF) and the magnetospheric magnetic field occurs at the magnetopause. This process transfers plasma and electromagnetic energy from the solar wind into the magnetosphere and drives large-scale convection of magnetic field lines in the magnetosphere-ionosphere system [Dungey, 1961]. Previous studies of magnetic reconnection have primarily focused on the local magnetic field configuration, such as the antiparallel reconnection hypothesis [Crooker, 1979] and the component reconnection hypothesis [Nishida and Maezawa, 1971; Sonnerup, 1974].

Here, we consider the corresponding vacuum magnetic field of the solar wind–magnetosphere system. First, we discuss the magnetic structure determined by the solenoidal condition, $\nabla \cdot \boldsymbol{B} = 0$. As a consequence, magnetic field lines cannot normally split or merge. Changes in magnetic connectivity can occur only at special locations where the magnetic-field direction, $\hat{e} = \boldsymbol{B}/|\boldsymbol{B}|$, becomes undefined. Such locations are magnetic null points. (As a side note, the magnetic-field direction is also undefined at singular points where the magnetic-field strength formally becomes infinite ($|\mathbf{B}| \to \infty$) at the center of a dipole magnetic field.) Therefore, magnetic null points play a crucial role in determining the magnetic connectivity and topology of the vacuum magnetic field. In other words, the solenoidal condition will control global magnetic field structure through the null points.

Next, let's consider the global structure of the corresponding vacuum magnetic field brought about by null points. The vacuum magnetic structure is given by the superposition of the Earth's magnetic field and the uniform IMF. We first show that this magnetic field generally contains two magnetic null points. Let

https://doi.org/10.5194/egusphere-2026-3829
Preprint. Discussion started: 25 August 2026

the Earth's magnetic field be represented by a dipole field with magnetic moment $(0,0,-m)$, where $m > 0$, and let the IMF be $(0, B_y, B_z)$ for simplicity. In this condition, any null point must be located in the y-z plane ($x = 0$). Accordingly, we denote the position of a null point by $(0, y_n, z_n)$. The null-point condition $\mathbf{B} = 0$ where $\boldsymbol{B}$ is a magnetic field vector, then yields

$$\frac{3y_n z_n}{r^5} - b_y = 0, \quad (1)$$

$$\frac{2z_n^2 - y_n^2}{r^5} - b_z = 0, \quad (2)$$

where

$$b_{y,z} = B_{y,z}\left(\frac{4\pi}{\mu_0 m}\right),$$

and

$$r = \sqrt{y_n^2 + z_n^2},$$

with μ_0 being the permeability of a vacuum.

Defining

$$\alpha = \frac{B_y}{B_z}$$

and eliminating r from Eqs. (1) and (2), we obtain

$$2\alpha z_n^2 - 3z_n y_n - \alpha y_n^2 = 0. \quad (3)$$

The solution of Eq. (3) is

$$z_n = \frac{3 \pm \sqrt{9 + 8\alpha^2}}{4\alpha} y_n. \quad (4)$$

For $b_y > 0$, Eq. (1) implies that $y_n z_n > 0$. Consequently, when $\alpha \neq 0$, the physically admissible solution of Eq. (4) corresponds to the positive branch, $+\sqrt{9 + 8\alpha^2}$. It follows that two null points exist: one with $y_n > 0$ and $z_n > 0$, and the other with $y_n < 0$ and $z_n < 0$. These two null points are located at positions symmetric with respect to the center of the dipole field. (Note that for a purely southward IMF ($\alpha = 0$ and $b_z < 0$), the magnetic field strength vanishes along a circle in the magnetic equatorial plane. In this degenerate case, the two null points merge into a continuous null line, and therefore isolated null points do not exist.)

Next, we show that magnetic null points play a fundamental role in determining the global magnetic-field structure of the corresponding vacuum field. The vacuum field contains both the Earth's dipole field and the IMF. Because magnetic connectivity can change only at the null points, the dipole field and the IMF are topologically connected through them. So, this gives rise to open magnetic field lines. Then, two types of open field lines are formed, connecting the IMF to the ionospheres of the Northern and Southern Hemispheres, respectively. Consequently, the boundary between the open- and closed-field-line regions on the ionosphere forms a closed curve. All field lines threading this boundary pass through the corresponding null point. Namely, this fact demonstrates that the null points control the connectivity between the magnetic domains. Thus, the global magnetic-field structure of the solar wind–

https://doi.org/10.5194/egusphere-2026-3829
Preprint. Discussion started: 25 August 2026

magnetosphere system is organized by the magnetic null points. The resulting field-line topology has been described previously by, for example, Lau and Finn (1990). As explained later, the superposition of the dipole magnetic field and a uniform IMF gives rise to a characteristic magnetic-field structure containing two null points. This structure forms the background magnetic-field configuration for global magnetic reconnection [e.g., Dorelli et al., 2007].

As mentioned at the beginning of this section, conventional explanations for the formation of the solar wind–magnetosphere structure assume that the magnetic-field structure is determined primarily by force balance, and that reconnection then occurs within the local topology formed by the IMF and the magnetospheric magnetic field. By contrast, because the vacuum magnetic field provides the background field for global reconnection, this raises the question of whether force balance and the topology of the vacuum magnetic field play equally important roles in determining the solar wind–magnetosphere structure. This question motivates the present study. Global magnetohydrodynamic (MHD) simulations self-consistently incorporate the interaction between magnetic fields and plasma. It is therefore useful to reinterpret the simulation results from the perspective of the interaction between the vacuum magnetic topology and plasma dynamics. In this paper we investigate this problem under oblique northward IMF conditions.

1.2 Previous research based on magnetic field topology

The main focus of this paper is to reconsider the magnetic field structure of the solar wind-magnetosphere system from the perspective of the interaction between magnetic topology and plasma dynamics. Therefore, a detailed investigation of the physical processes of global magnetic reconnection is beyond the scope of the present study. However, the corresponding vacuum magnetic field has been extensively used to investigate three-dimensional (3D) global magnetic reconnection, particularly under northward IMF conditions [e.g., Cowley, 1973; Siscoe, 1988; Lau and Finn, 1990; Crooker et al., 1998; Siscoe et al., 2001; Dorelli et al., 2007]. Moreover, magnetic-field convection driven by global reconnection in the magnetosphere–ionosphere system influences the large-scale magnetic-field structure of the magnetosphere. Therefore, before proceeding further, we review previous studies of global magnetic reconnection based on vacuum magnetic-field topology. We also briefly introduce several studies that have interpreted global magnetospheric phenomena from the perspective of magnetic topology.

Widely accepted studies on the structure and physical processes of the steady solar wind–magnetosphere system were initiated by Dungey (1961, 1962). He first proposed the open magnetosphere model in which magnetic reconnection at the magnetopause drives steady magnetosphere-ionosphere convection. Furthermore, Dungey (1962) addressed the problem of 3D magnetic reconnection between the IMF and the magnetospheric magnetic field. He emphasized that null points, where the magnetic field strength vanishes, play an essential role in 3D magnetic reconnection.

https://doi.org/10.5194/egusphere-2026-3829
Preprint. Discussion started: 25 August 2026

Following Dungey (1962), Cowley (1973) qualitatively discussed three-dimensional global magnetic reconnection at the solar wind–magnetosphere interface using the vacuum magnetic field formed by the superposition of a uniform interplanetary magnetic field (IMF) and the Earth's main magnetic field, which contains two null points in the Northern and Southern Hemispheres. He pointed out that magnetic field lines belonging to different topological domains coincide on a special field line connecting the two null points (called the separator), and argued that the separator plays an important role in global reconnection. Stimulated by the quantitative discussion by Cowley (1973), many theoretical and simulation studies of the physical processes in the solar wind–magnetosphere system have focused on the nature of 3D global magnetic reconnection by using either the vacuum field [e.g., Cowley, 1973; Stern, 1973; Crooker, 1979; Greene, 1988; Lau and Finn, 1990; Wang and Bhattacherjee, 1996] - or realistic magnetic fields in the solar wind environment derived from global MHD simulations [e.g., Crooker et al., 1998; Siscoe et al., 2000, 2001; Dorelli et al., 2007]. Furthermore, in the context of general 3D magnetic reconnection, Hesse and Schindler (1988) showed that the existence of an electric field parallel to the magnetic field - namely, a finite potential drop along magnetic field lines - is essential for reconnection. In this framework, null points or separators are not strictly required for reconnection to occur. This concept provides a fundamental description of the 3D magnetic reconnection. By synthesizing the work of Cowley (1973) and Hesse and Schindler (1988), Lau and Finn (1990) studied the 3D global reconnection in a theoretical way. To discussing the reconnection, they described the characteristic magnetic field structures associated with magnetic topology near null points based on the solenoidal condition ($\nabla \cdot \boldsymbol{B} = 0$). Finally, Lau and Finn (1990) clearly demonstrated that magnetic reconnection can be understood as a change in magnetic field line connectivity caused by non-ideal MHD effects localized along separators.

Recent simulations have enabled the precise solution of the MHD process in the solar wind–magnetosphere region. Dorelli et al. (2007) investigated the separator reconnection [Lau and Finn, 1990; Priest and Forbes, 2000] at the dayside magnetopause using global MHD simulations of the solar wind–magnetosphere system. They were focused on the reconnection under obliquely northward IMF conditions. They further showed that null points are not mathematically idealized points, as assumed in the theoretical treatment of Lau and Finn (1990), but instead form a spatially distributed cluster of nulls. Nevertheless, from a global perspective, the magnetic topology of the solar wind–magnetosphere system remains largely unchanged from that of the corresponding vacuum magnetic field. In addition, the null points remain located near their original vacuum-field positions despite the deformation of the magnetic field by the solar-wind plasma. Moreover, they found that the separator reconnection exhibits characteristics of component reconnection [e.g., Sonnerup, 1974] in the equatorial region, while showing features similar to anti-parallel reconnection [e.g., Crooker, 1979] near the high-latitude null points. As a summary, in separator reconnection, the reconnection of magnetic field lines manifests as a discontinuous change in their footpoint connections as the field lines pass through a localized region of field-aligned electric field distributed along the separator. The null point represents the boundary of magnetic topology,

https://doi.org/10.5194/egusphere-2026-3829
Preprint. Discussion started: 25 August 2026

where magnetic field lines branch into areas of different connectivity; however, it is not necessarily the site where magnetic reconnection (i.e., connectivity change) itself occurs [Hesse and Schindler, 1988; Lau and Finn, 1990; Priest and Forbes, 2000; Dorelli et al., 2007]. It should be noted that previous MHD simulation studies of global magnetic reconnection have generally focused on the reconnection process itself, rather than on the global magnetic-field structure and the plasma dynamics within that structure.

For the issue of the magnetic diffusion necessary for the global reconnection, Stern (1973) argued that the global magnetic field structure with the null point always accompanies diffusion. That is to say, the open-closed boundary magnetic field lines have footpoints in the ionosphere of the Southern (Northern) Hemisphere. At the same time, they converge at the null points in the Northern (Southern) Hemisphere. Moreover, the ionospheric potential is not constant along the open-closed boundary in the ionosphere. Therefore, if the magnetic field lines are equipotential, the electric field will diverge to infinity at the null point, reflecting the potential difference in the ionosphere. Therefore, electric resistivity along the magnetic field lines is required near the null point. As a result, this resistivity becomes the non-MHD effect causing the magnetic diffusion. Siscoe et al. (2001) confirmed, using resistive MHD simulations, that a field-aligned electric field, required for 3D global magnetic reconnection as demonstrated by Hesse and Schindler (1988), appears along separators as proposed by Stern (1973).

Regarding the relationship between plasma dynamics and global magnetic topology, Stern (1973) qualitatively studied plasma behavior in a vacuum magnetic field deformed by the solar wind. His research dealt with the interaction between the magnetic topology and plasma dynamical processes in a qualitative manner. He found that the solar wind plasma can enter the magnetotail via a “window” created on the flank side of the magnetotail after the work of Morfill and Schorer (1972). However, because supercomputer facilities were not available at the time, it was difficult to accurately calculate the complex interactions in 3D space and study their physical mechanisms. After Stern (1973), research into the interaction of magnetic topology and plasma dynamics seems to have slowed down, probably because the work of Dungey (1961) was so convincing.

Other studies on the relationship between global phenomena and the magnetic topology in the solar wind–magnetosphere system have focused on 3D magnetic field convection in the magnetosphere-ionosphere region [Tanaka, 1999; Watanabe et al., 2005, 2007, 2010; Tanaka, 2007; Tanaka et al., 2017, 2019, 2024]. For example, because the magnetic field lines connecting the ionosphere and magnetosphere are equipotential, Tanaka (1999) showed the 3D magnetic field convection in the magnetosphere that corresponds to the ionospheric convection in the obliquely northward IMF condition. He also argued that the magnetic field line of the solar wind and that of the magnetosphere switch connections at the null point. Watanabe et al. (2005) argued that magnetic convection occurs in a magnetic field configuration with the same topology as that of the vacuum magnetic field. Tanaka et al. (2017) investigated the relationship among three factors: the magnetic field structure of a specific topology, the magnetospheric

https://doi.org/10.5194/egusphere-2026-3829
Preprint. Discussion started: 25 August 2026

plasma distribution, and the ionospheric field-aligned current (FAC) distribution under the condition of the northward IMF with a negative By. They showed that the open-closed field line boundaries in the ionosphere correspond to distinct auroral features. Specifically, the high-latitude boundaries match the Horse Collar aurora [Hones et al., 1989], and the low-latitude boundaries correspond to the polar slot (void). These findings demonstrated a direct connection between auroral structures and the magnetic topology. However, the analysis was largely limited to structures projected onto the ionosphere. As a result, further investigations is required for the global topology of the solar wind–magnetosphere system. More recently, Tanaka et al. (2024) summarized the relationship between magnetosphere-ionosphere convection systems and magnetic branching at the null points associated with this topology. On the other hand, the processes that generate magnetic-field structures and plasma behavior in the solar wind–magnetosphere system remain insufficiently understood from the perspective of the interaction between magnetic topology and plasma dynamics. Therefore, we need more effort to elucidate the physical process.

As mentioned earlier, it is already known that topology with two nulls and two separators is conserved in the solar wind environment, but it is not clear exactly why and how the magnetic field is deformed. This is a study that quantitatively builds upon Stern's research. In other words, it is necessary to consider the solar wind–magnetosphere system from the perspective of the interaction between magnetic topology and plasma dynamics using global simulation data. Therefore, this paper mainly examines the magnetic field structure of the solar wind–magnetosphere system and the physical mechanism of its generation under obliquely northward IMF conditions. The plasma behavior including the plasma distribution, convection, bulk flow patterns, and current systems driven by this interaction will be discussed in the other paper.

1.3 Structure of this paper

The structure of the remainder of the present paper is as follows. First, in Sect. 2, we explain how we consider the physical process in the solar wind–magnetosphere system as the interaction between the magnetic topology and plasma dynamics to reveal the fundamental principles that determine the structure of the solar wind–magnetosphere system. The magnetic topology and its specific magnetic field line structure will also be explained in detail. Section 3 briefly describes the numerical code used for this research. Next, in Sect. 4, we illustrate the shape of the open-closed field boundary (the torus) and the IMF-open field boundary (the cylinder) by using the vacuum magnetic field and the field modified by the solar wind. Based on the illustrations, we clarify the role of the fundamental physical laws introduced in Sect. 2. Section 5 discusses the role of the magnetic field convection associated with the global magnetic reconnection and the possible reason why the magnetic topology is conserved. Section 6 summarizes the main results of this study.

https://doi.org/10.5194/egusphere-2026-3829
Preprint. Discussion started: 25 August 2026

2 Fundamental physical processes in the quasi-steady solar wind-magnetosphere system

2.1 Key processes of formation of the solar wind–magnetosphere system

The purpose of this paper is to clarify how the magnetic field structure of the solar wind–magnetosphere system is deformed by the solar wind through the interaction of plasma dynamics and magnetic topology under obliquely northward IMF conditions. In order to understand this interaction, we first need to consider how to treat the physical processes of the solar wind–magnetosphere system.

The magnetic topology of the solar wind–magnetosphere system is defined by the connectivity of magnetic field lines when the solar wind and the magnetosphere are regarded as a single system. Because magnetospheric plasma is predominantly of solar-wind origin, the global dynamics of this coupled system are commonly investigated using global magnetohydrodynamic (MHD) simulations based on the one-fluid approximation. Therefore, to investigate the relationship between magnetic topology and plasma dynamics, we will use the global MHD simulations. The background magnetic field, denoted by $\boldsymbol{B}_0$, is given by the superposition of the Earth's main magnetic field and the uniform IMF, whereas the magnetic field generated by plasma currents is denoted by $\boldsymbol{B}_1$. Following Raeder et al. (1998), the MHD equations can be written as

$$\frac{\partial \rho}{\partial t} + \nabla \cdot (\rho \boldsymbol{v}) = 0, \tag{5}$$

$$\rho \left[\frac{\partial \boldsymbol{v}}{\partial t} + (\boldsymbol{v} \cdot \nabla)\boldsymbol{v}\right] + \nabla p = \left(\frac{\nabla \times \boldsymbol{B}_1}{\mu_0}\right) \times (\boldsymbol{B}_0 + \boldsymbol{B}_1), \tag{6}$$

$$\frac{\partial \epsilon}{\partial t} + \nabla \cdot \{(\epsilon + p)\boldsymbol{v}\} = \left(\frac{\nabla \times \boldsymbol{B}_1}{\mu_0}\right) \cdot \boldsymbol{E}, \tag{7}$$

$$\frac{\partial \boldsymbol{B}_1}{\partial t} = -\nabla \times \boldsymbol{E}, \tag{8}$$

$$\boldsymbol{E} + \boldsymbol{v} \times (\boldsymbol{B}_0 + \boldsymbol{B}_1) = \eta \frac{\nabla \times \boldsymbol{B}_1}{\mu_0}, \tag{9}$$

where ρ, $\boldsymbol{v}$, p, $\boldsymbol{E}$, and ϵ in these equations are, respectively, plasma density, plasma velocity, thermal plasma pressure, electric field, the internal energy ($\epsilon = \frac{\rho v^2}{2} + p/(\gamma - 1)$ where γ is the polytropic index). In addition, η is the resistivity. Thus, Eq. (5) and the left-hand sides of Eqs. (6) and (7) describe the fluid dynamics of the plasma and correspond to the equations of gas dynamics. In contrast, Equation (8), together with the right-hand sides of Eqs. (6) and (7), constitutes the magnetic part of the MHD equations and describes the influence of both the background magnetic field and the magnetic field generated by plasma currents on the plasma dynamics. Equation (9) is the well-known frozen-in condition of ideal MHD, which governs the evolution of magnetic field lines in response to plasma motion. From the viewpoint that the MHD equations describe the interaction between plasma dynamics and magnetic fields, the frozen-in condition may be regarded as a fundamental constraint on this interaction.

Before examining the results of the global MHD simulations, it is useful to consider the implications of Eqs. (5)–(9) through a series of thought experiments. To elucidate the fundamental physics of a system governed by the interaction of two components, it is often instructive to examine limiting cases in which

https://doi.org/10.5194/egusphere-2026-3829
Preprint. Discussion started: 25 August 2026

only one component is present. Following this approach, we consider qualitatively two idealized limiting cases of the solar wind–magnetosphere system: (1) a vacuum state in which only the magnetic field exists and the plasma is absent, and (2) an unmagnetized state in which only the plasma exists and the magnetic field is absent.

Let's consider case (1). In this case, $\boldsymbol{B}_1 = \boldsymbol{E} = \boldsymbol{v} = 0$. So, there remains only the background magnetic field. This state has two important implications for understanding the physical processes of the solar wind–magnetosphere system from the perspectives of magnetic topology and the plasma dynamics. First, as the perspective of magnetic topology, the magnetic field of this system becomes a vacuum magnetic field, specifically a superposition of the Earth's main magnetic field and a uniform IMF as noticed previously. The magnetic field structure is shown in Fig. 1A. This figure is a redraw of Fig. 5(b) from Lau and Finn (1990), viewed from the afternoon side, assuming a dipole main magnetic field and an IMF in the obliquely northwest direction (IMFBz > 0, IMFby < 0). This IMF condition will be denoted as IMFz + By- from now on. It is noteworthy that this magnetic structure possesses a specific topology that allows for global magnetic reconnection [e.g., Lau and Finn, 1990]. Second, from the perspective of the dynamical processes, since the Earth's main magnetic field and a uniform IMF are potential magnetic fields, $\nabla \times \boldsymbol{B}_0 = 0$ holds. Therefore, no current ($\boldsymbol{J}$) flows under this condition. Generally, the Lorentz force in plasma can be decomposed as follows,

$$\boldsymbol{J}_\perp \times \boldsymbol{B} = -\frac{\nabla|\boldsymbol{B}|^2}{2\mu_0} + \frac{|\boldsymbol{B}|^2(\hat{e}\cdot\nabla)\hat{e}}{\mu_0}. \quad (10)$$

The first and the second terms on the right-hand side of this equation represent the magnetic pressure gradient force and magnetic tension force, respectively. (Vectors with the subscript $\perp$ indicate components perpendicular to the magnetic field lines.) Equation (10) shows that in a potential magnetic field where $\boldsymbol{J} = 0$, the magnetic pressure gradient and magnetic tension are balanced, and no force is generated. Therefore, the vacuum magnetic field is the magnetic field with the lowest magnetic field energy. Based solely on this discussion, it would seem that when a magnetic field is deformed from the vacuum field by an external force, a Lorentz force appears as a restoring force, causing the magnetic field to tend to return to the vacuum field. However, the magnetic flux transported toward the nightside magnetotail by the magnetic convection also contributes to generation of the Lorentz force. The resulting Lorentz force also plays a role in counteracting an external force. The restoring force that attempts to return to the vacuum magnetic field and the force created by the magnetic flux carried by convection may vary in relative magnitude depending on the location in the magnetotail. For example, where the former is dominant, the magnetic field structure will tend to conform to the vacuum magnetic field. These will be investigated using numerical calculations.

In case (2), the supersonic solar-wind plasma flow would pass the obstacle (the Earth) almost ballistically and form a wake downstream the obstacle in the solar wind–magnetosphere system as shown in Fig. 1B, similar to Venus and Mars [i.e., Lundin and Barabash, 2011]. Therefore, inside the daytime

https://doi.org/10.5194/egusphere-2026-3829
Preprint. Discussion started: 25 August 2026

bow shock, plasma would be compressed, and in regions far from Earth, the pressure would decrease as the cross-sectional area enclosed by the bow shock expands. (Strictly speaking, the gas-dynamic flow around an obstacle is not identical to that around Venus and Mars because the IMF is present in the actual solar wind. However, because the Alfvén Mach number in the vicinity of the Earth is generally greater than unity, the IMF does not significantly affect the plasma flow around the obstacle.)

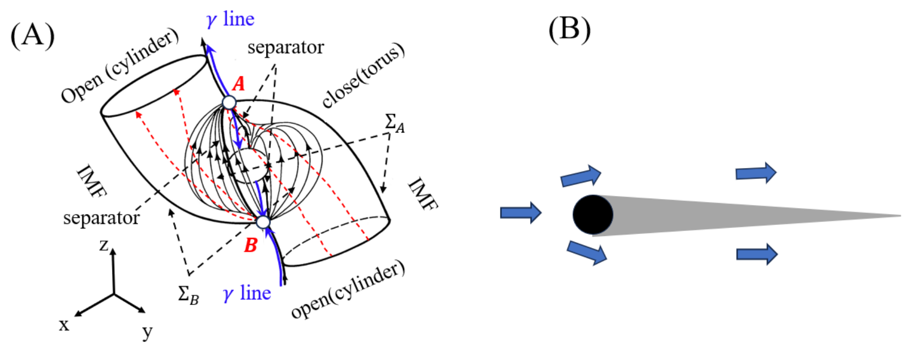

Fig. 1. (A) Schematic view of the plasma-free magnetic field as viewed from the afternoon sector. It represents the superposition of the Earth's dipole field and a uniform IMF with + Bz and - By. The three axes (x, y, and z) shown in the lower-left corner denote the sunward, eastward, and northward directions, respectively. This figure provides an alternate perspective on Figure 5(b) of Lau and Finn (1990). The black and blue curves with thick arrows indicate the separators and γ lines, respectively. The red dashed lines indicate the magnetic field lines at the IMF-open field boundary. See the text for a detailed explanation. (B) Thought experiment illustrating a plasma distribution produced solely by the solar wind flow in the absence of a magnetic field. A cone-shaped shadow is expected to form behind Earth; however, such a structure is not stable.

The actual solar wind–magnetosphere system may be regarded as an intermediate state between cases (1) and (2), established through a force balance between the Lorentz force and the plasma forces. In addition, the magnetic flux transported into the magnetosphere by the global reconnection further modifies this force balance. In this paper, we refer to this conceptual framework based on the above force balance as the *mechanical principle*. This principle provides a fundamental basis for understanding the structure of the steady-state solar wind–magnetosphere system.

We next consider the magnetic topology. In the plasma-free limit, i.e., the background vacuum magnetic field, the magnetic topology shown in Fig. 1A emerges. Moreover, global MHD simulations have confirmed that this topology is almost preserved in the solar wind environment under obliquely northward IMF conditions [e.g., Watanabe et al., 2005; Tanaka et al., 2017; Xiong et al., 2024]. However, it is noted

https://doi.org/10.5194/egusphere-2026-3829
Preprint. Discussion started: 25 August 2026

that the simulation results do not completely preserve the topology of the vacuum magnetic field. Specifically, Dorelli et al. (2007) used their simulation results to show that null points are not mathematically idealized points, but rather form clusters of null points with a finite spatial extent. Nevertheless, they also showed that, at the global scale, the overall topological structure of the vacuum magnetic field does not change even in the presence of solar wind. Therefore, the fact that the topology does not change even when the vacuum magnetic field is deformed by the solar wind holds true on a global scale. Hereafter, this regulation is referred to as the *topology conservation property*. Furthermore, this property also implicitly includes the fact that the null points do not significantly deviate from their original positions in the skeletal field. This will be explained in Sect. 4.1.

As explained previously, the background vacuum magnetic field represents the lowest magnetic energy state. Therefore, ignoring the effects of reconnection, this state is the most stable state of the solar wind–magnetosphere system. Furthermore, the simulation results showing that the magnetic topology of the vacuum magnetic field is preserved under the solar wind plasma conditions suggests that the structure of the solar wind–magnetosphere system is strongly constrained by the vacuum magnetic field, even with the effects of global magnetic reconnection. (In this sense, although not physically accurate because the vacuum field does not consider the ionosphere nor transport of the magnetic flux via global reconnection, it is not entirely wrong to call the vacuum magnetic field the "ground state" of the solar wind–magnetosphere system.)

In summary, the mechanical principle and the topology conservation property together provide a unified framework that governs the magnetic field structure and plasma behavior in the quasi-steady solar wind–magnetosphere system under steady solar wind conditions with the obliquely northward IMF conditions.

2.2 Magnetic-field structure associated with the topology

This study focuses on the magnetic-field structure associated with the particular topology in order to elucidate the interaction between magnetic topology and plasma dynamics. A clear understanding of the vacuum magnetic topology and its associated field-line structure is essential for interpreting the results presented later. Here, based on the work of Lau and Finn (1990), we will explain the structure by using Fig. 1A. This figure shows that two magnetic null points appear symmetrically about the center of Earth: one in the Northern Hemisphere (a convergent null, denoted as A) and the other in the Southern Hemisphere (a divergent null, denoted as B). Because of the solenoidal condition of the magnetic field, magnetic field lines generally do not branch. Branching occurs only at null points where the magnetic field strength vanishes. In this case, a group of converging or diverging field lines focused on the null point forms a surface. This surface serves as a boundary separating magnetic fields of different origins and topologies. This surface is called the Σ surface [Lau and Finn, 1990] or the fan [Craig et al., 1997]. The surfaces formed by magnetic field lines converging to the null point A and diverging from the null point B are referred to as the Σ_A and Σ_B surfaces, respectively, in this paper. Whereas, the intersection

https://doi.org/10.5194/egusphere-2026-3829
Preprint. Discussion started: 25 August 2026

lines of the Σ_A surface and the Σ_B surface become magnetic field lines connecting the two nulls. These connecting field lines, which appear on both the dayside and nightside, are called separators. Furthermore, each Σ surface has a part of the open-closed boundary and the open-IMF boundary. The magnetic field lines passing the open-closed boundary in the Southern (Northern) Hemisphere all have foci at null point A (B), and therefore belong to the Σ_A (Σ_B) surface. The two surfaces formed by these two open-close boundary field lines together form a *torus* [Siscoe et al., 2001; Watanabe et al., 2005]. The torus parts of the Σ_A and Σ_B surfaces are separated by the separator. In contrast, the open-IMF boundary forms two *cylinders*, which gradually extend along the IMF as they move away from Earth [Siscoe et al., 2001; Watanabe et al., 2005]. The intersection of the torus and cylinder on the same Σ surface is the separator. Therefore, the separator represents the intersection of four distinct magnetic field line topologies: (i) closed field lines confined within the magnetosphere (torus), (ii) open field lines connecting the ionosphere of the Northern Hemisphere to the IMF (cylinder), (iii) open field lines connecting the ionosphere of the Southern Hemisphere to the IMF (cylinder), and (iv) the IMF itself. Furthermore, to satisfy $\nabla \cdot \boldsymbol{B} = 0$ (the solenoidal condition) at null points, pairs of singular magnetic field lines must emanate from or converge into each null point, corresponding to the convergence or divergence of the field lines belonging to the Σ surface. These field lines are called γ lines [Lau and Finn, 1990] or the spine [Craig et al., 1997]. In addition, one of the γ lines that connect the null points directly to the ionosphere are termed *stem lines* [Siscoe et al., 2001]. A key property is that the subset of γ_A lines extending from null point A to the IMF lies on the Σ_B surface, whereas the subset of γ_B lines extending from null point B to the IMF lies on the Σ_A surface (see Fig. 5 of Dorelli et al., 2007, or Fig. 8.8(b) of Priest and Forbes, 2000). This geometric property of the γ lines gives rise to a distinctive solar wind–magnetosphere structure, as discussed later in Sect. 4.1.2. The same geometric relationship is also evident in the magnetic-field topology of the solar wind–magnetosphere system shown in Fig. 1A. Unlike the magnetic configuration discussed by Fig. 5 of Dorelli et al. (2007), which contains only one separator, the solar wind–magnetosphere system contains two separators connecting null points A and B: one passing through the dayside and the other through the nightside. Both separators lie on the fan surfaces Σ_A and Σ_B. Of the two spines (γ lines) extending from null point A, one connects to the IMF along the cylinder branch of the Σ_B surface, whereas the other extends from null point A to the open–closed boundary in the northern ionosphere and forms the stem line. All other field lines on the open–closed boundary in the northern ionosphere pass through null point B and therefore belong to the Σ_B surface.

Thus, the vacuum magnetic topology of the solar wind–magnetosphere system is characterized by two null points and two separators, referred to as the null-separator structure [Watanabe et al., 2005] or the two-null, two-separator structure [Tanaka et al., 2018; Xiong et al., 2024].

Together, null points and separators constitute the fundamental elements defining the magnetic topology of this structure. On the other hand, under due-north IMF conditions, the null points are located on the z-axis, and the magnetic field configuration is axisymmetric about the z-axis. In this case, there are

https://doi.org/10.5194/egusphere-2026-3829
Preprint. Discussion started: 25 August 2026

infinitely many lines connecting the two null points, so the separator forms a surface. As a result, the magnetic topology under the due-north IMF condition is fundamentally different from that for obliquely northward IMF conditions. Accordingly, the present study focuses on obliquely northward IMF conditions but excludes the due-north IMF case.

The vacuum magnetic field has three characteristic features: 1) it inherently possesses a magnetic field configuration that incorporates global magnetic reconnection; 2) it is related to the minimum magnetic field energy state of the solar wind–magnetosphere system; 3) it appears when plasma is removed. Considering these characteristic features, it is appropriate to call the vacuum magnetic field the skeletal magnetic field of this system. Throughout the latter part of the present paper, the vacuum magnetic field structure will be referred to as the skeletal magnetic field structure, or simply the skeletal structure. (Please note that the word “skeleton” refers to the regime boundary of the magnetic field in solar physics [Li Ting et al., 2021]. We use this term in a different sense in the present paper.)

3 Model and Simulation

The present simulation study used the global MHD simulation code named REProduce Plasma Universe (REPPU), developed by Tanaka (2015). This code solves the MHD equations in the solar wind–magnetosphere region. The inner boundary of the MHD simulation domain (the magnetosphere) is set at r = 3 R_E. The outer boundaries of the magnetosphere are located at 600 R_E on the dayside and 200 R_E on the nightside. The grid structure used by REPPU is almost spherical near Earth, but is designed to approximate cylindrical coordinates in the nightside magnetotail. That is to say, the center of the coordinates shifts slightly toward the Sun as the radius increases, as shown in Fig. 5 of Moriguchi et al. (2008). This allows for a more finely spaced grid to be placed in the nightside magnetotail region. (This grid structure is employed to perform highly accurate calculations of the nightside plasma sheet phenomenon, which plays an important role in magnetospheric physics.)

The FAC at the inner boundary of the simulation domain (3 R_E) is projected to the ionosphere (r = 1 R_E) along the dipole magnetic field. The electric field induced in the conductive ionosphere by the FAC is again projected to the inner boundary of the magnetosphere along the dipole magnetic field, assuming the equipotential of the field lines. The ionospheric conductivity is determined by the FAC and plasma temperature and pressure at the inner boundary of the magnetosphere to reproduce the realistic ionospheric conductivity depending on the magnetospheric activity [Tanaka et al., 2010]. The level 6 version of the REPPU code that we employed for this study has 61,440 triangular surface cells on one sphere and 240 radial layers, for a total of 14,745,600 grid elements. (The horizontal mesh size is about 0.1 R_E on a sphere of r = 10 R_E, and the distance between the spheres is about 0.2 R_E.) The solar wind is injected into the plane at x = 25 R_E upstream of Earth. The solar wind parameters used in this study are as follows: plasma density of 10cm^{-3}, IMF = (Bx = 0 nT, By = -4.3 nT, Bz = 4.3 nT) (IMFBz+By-), V_x = 372

https://doi.org/10.5194/egusphere-2026-3829
Preprint. Discussion started: 25 August 2026

km/sec, $V_y = V_z = 0$ km/sec, and a solar wind temperature of 3,000,000 K. The simulation results are the same as those used by Xiong et al. (2024) for their topological analysis.

The solar wind–magnetosphere system in global MHD simulations is known not to remain perfectly steady even under the northward IMF condition with constant solar wind parameters. For instance, the simulation results always include small fluctuations. However, we confirmed that the solar wind–magnetosphere system exhibits a structure with the same topology as the magnetic field structure of the null-separator shown in Fig. 1. (The simulation results shown in Sect. 4 will confirm that the topology is conserved.) In this study, we analyzed the simulation data 132.5 minutes after plasma was injected into the skeletal magnetic field. The solar wind–magnetosphere at this time exhibits a typical, quasi-steady behavior under the northward IMF condition.

4 Deformation of the Magnetic Field Structure based on the Mechanical Principle and the Topology Conservation Property

As explained in the previous section, the magnetic topology of the skeletal magnetic field is conserved even in the real solar wind–magnetosphere system, where the magnetic field is deformed by the solar wind. In other words, the skeletal field changes its geometry while preserving its topology. However, understanding of the detailed configuration of the deformed magnetic field lines and the physical processes responsible for the deformation remains incomplete. In this section, we examine how the mechanical principle and the topology conservation property govern the deformation of the skeletal magnetic field by the solar wind. Our analysis focused on the deformation of two specific structures: the cylinder, which corresponds to the magnetotail, and the torus whose nighttime part is roughly corresponds to the plasma sheet.

To analyze how the solar wind deforms the skeletal magnetic field, it is helpful to compare the deformed magnetic field structure with the original skeletal one under the identical IMF condition. For this, we show magnetic field lines on the cylinder and torus for both the skeletal and deformed fields. This section highlights the main features of these magnetic field structures and explores the physical mechanisms behind the deformation, focusing on the interaction between the magnetic topology and plasma dynamical processes.

The deformed field is obtained from the REPPU simulation. Considering the result by Dorelli et al. (2007) that multiple magnetic null points intermittently appear even under steady obliquely northward IMF conditions, it is inferred that the solar wind–magnetosphere system exhibits small intrinsic fluctuations even when the IMF is steady and northward. As a consequence, the magnetic field lines obtained from the REPPU simulation are, strictly speaking, accompanied by small temporal fluctuations. Therefore, the magnetic field configuration presented in this paper should be regarded, in a strict sense, as

https://doi.org/10.5194/egusphere-2026-3829
Preprint. Discussion started: 25 August 2026

a snapshot at a particular time. Nevertheless, except for exceptional cases discussed in Sect. 5.2, these fluctuations do not invalidate the existence of the null-separator structure.

Because the null points play a critical role in determining the magnetic field structure in the solar wind–magnetosphere system, we first identified the null points from the numerical simulation results. For deformed magnetic fields, we employed the method proposed by Haynes and Parnell (2007). First, we assumed the existence of null points where the magnetic field vectors at computational grid points exhibit convergent or divergent behavior. A null point was identified when the minimum magnetic field strength within the grid was less than 0.04 nT. Dorelli et al. (2007) indicated that a null point cluster appears just downstream of the most upstream null point. We also found such a cluster in the deformed magnetic field line structure. The null points in this cluster flicker and fluctuate, but the upstream-most null points, which appear in the Northern and Southern Hemispheres, remain nearly stationary. Therefore, after Dorelli et al. (2007), we draw the dayside and nightside separators using the stationary null points that appear farthest upstream. Meanwhile, the null points of the skeletal magnetic field structure are determined as points with a magnetic strength less than 0.5 nT using a graphic processing code, without relying on rigorous numerical calculations, because the magnetic strength distribution is smooth. The null points in the Northern and Southern Hemispheres are denoted as A and B, respectively, to match the notation of Fig. 1A.

4.1 Deformation of the Cylinder

We here first examine the cylinder part of the Σ_A surface (the magnetic field lines connecting the northern ionosphere and IMF) for the IMFBz+By- condition. This cylinder is defined as a bundle of magnetic field lines that converge at null point A in the Northern Hemisphere. It forms the boundary surface between the IMF and the region of open field lines. Figures 2A and 2B display the magnetic field lines on the skeletal cylinder part of the Σ_A surface as viewed from the Sun and 18 Magnetic Local Time (MLT), respectively. In contrast, Figures 2C and 2D show a snapshot of the magnetic field lines on the deformed cylinder observed from the same perspectives. The black dots in all panels of Fig. 2 indicate the locations of null points. In the skeletal case, the null points are located on the 06-18 MLT meridian plane. In the deformed magnetic field, the null points are still approximately in the 06-18 MLT meridional plane, but slightly displaced from their positions in the skeletal field, shifting closer to the dipole axis. Finally, Figure 2 shows that both the skeletal field and the deformation field exhibit a two-null, two-separator structure, and that the null points of both appear in approximately the same location. Thus, not only is the magnetic topology maintained under the influence of the solar wind, but the position of null points also does not change significantly. This result demonstrates the topology conservation property.

Note that, while the magnetic field lines on the cylinder part of the Σ_A surface are expected to converge precisely at null point A, some field lines shown in Fig. 2 exhibit slight deviations. This discrepancy arises from the simplified numerical method used to trace the outermost open field lines. However, this

https://doi.org/10.5194/egusphere-2026-3829
Preprint. Discussion started: 25 August 2026

deviation does not significantly affect the interpretation of the global magnetic field structure. A similar issue occurs in the calculation of the torus surface presented in Fig. 4. It should be noted that, using the same simulation dataset together with an improved tracing algorithm, Xion et al. (2024) demonstrated the accurate convergence of the Σ_A torus surface to the null point A. This result was obtained by applying a highly advanced numerical method. This result guarantees that all field lines on the regime boundary are essentially focused on the null point.

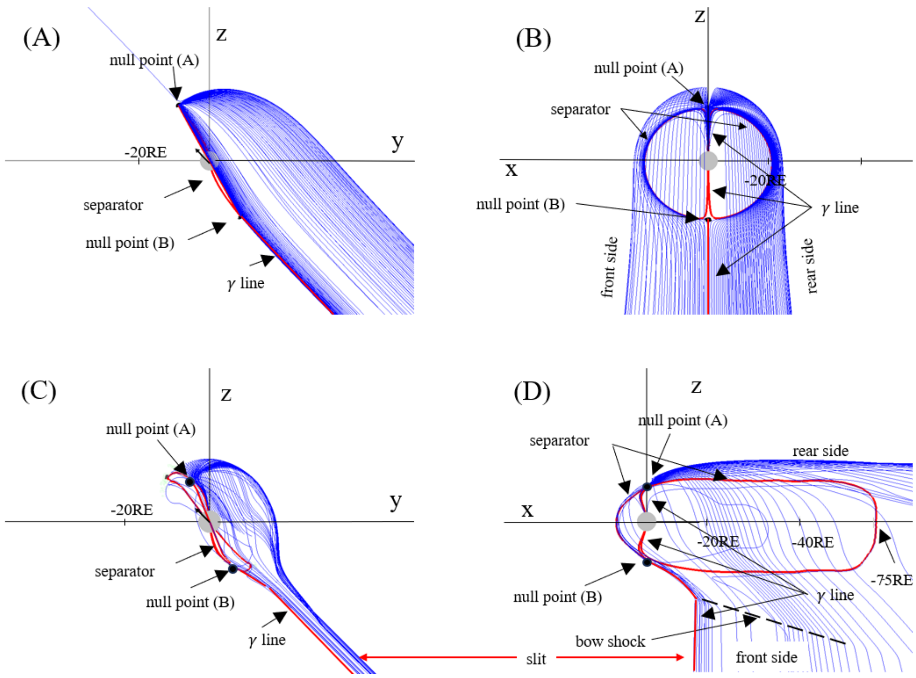

Fig. 2. Blue bundles of numerically calculated magnetic field lines depicting the skeletal cylinder part of the Σ_A surface in panel A, seen from the Sun, and panel B, seen from 18 MLT. The deformed cylinder part of the Σ_A surface from the Sun and 18 MLT are shown in panels C and D, respectively. The black dots labeled A and B correspond to null points A and B, respectively. The red bold curves that connect the two null points are the separator lines. The other bold red curves are the γ lines. The x, y, and z axes point sunward, eastward, and northward, respectively. The shape of the cylinder is symmetric concerning the y-z plane in the skeletal structure, as shown in panel B. In contrast, the deformed one has a slit extending toward the anti-sunward direction, as shown in panels C and D. The black dashed line in panel D shows the position of the bow shock. In panel D, the night-side separator crosses the equator at x ~ -75 R_E.

https://doi.org/10.5194/egusphere-2026-3829
Preprint. Discussion started: 25 August 2026

Based on the identified null points, we manually draw the dayside and nightside separators as bold red curves connecting the two null points across both hemispheres in Fig. 2. In addition, we plot the γ line, a stem field line connecting null point A to the ionosphere, as a bold red curve. Another γ line, extending from null point B and connecting to the IMF, is also illustrated with a bold red curve.

In the latter part of this paper, the upstream side (dayside) and downstream side (nightside) of the cylinder part of the Σ_A surface will be referred respectively to as the front side and the rear side, as indicated in Figs. 2B and 2D. More precisely, for the cylinder part of the Σ_A surface shown in Fig. 2, the magnetic field lines on the rear side originate in the IMF, approach null point A from the nightside, and converge there. Furthermore, they pass through the evening $(+y)$ side of the nightside separator. In contrast, the magnetic field lines on the front side originate from the IMF, pass near null point B and the dayside separator, and converge at null point A via the dusk side (+y side) of the day-side magnetopause. Extending this definition to the cylinder part of the Σ_B surface inclusive, the rear-side field lines are those connecting a null point to the nightside magnetotail, whereas the front-side field lines are those that pass through the null point, the regions near the dayside separator and near the other null point before connecting to the IMF. The boundary field line of the front side passes through the dayside separator and connects the null point to the other null point. The cylinder parts of the Σ_A and Σ_B surfaces are located on the afternoon and morning sides, respectively, of the plane defined by the dayside and nightside separators.

4.1.1 Magnetic Field Structure of the Magnetotail as a Manifestation of the Mechanical Principle

This section discusses the magnetic field structure on the rear side of the cylinder (the magnetotail), dividing it into two regions: 1) the near-Earth and mid-distance magnetotail (within 100 R_E of the Earth); 2) the distant magnetotail. The topology conservation property only requires that the magnetic field lines on the rear side pass through null point A. Therefore, the field lines connecting from the null point A to the IMF follow the mechanical principle.

First, we investigate deformation of the skeletal cylinder on the rear side in the near-Earth and mid-distance magnetotail. Figure 2B shows both the skeletal cylinder part of the Σ_A surface and the magnetic field lines on the cylinder surface extending predominantly in the z-direction (i.e., IMF direction) when viewed from 18 MLT. In contrast, Figure 2D shows that, on the rear side of the deformed Σ_A cylinder, the magnetic field lines retain only a small IMF-aligned component and are nearly aligned with the solar-wind flow direction $(-x)$. Furthermore, the envelope formed by these field lines is elongated in the Sun-Earth (x) direction. Thus, when viewed from 18 MLT, the skeletal Σ_A cylinder appears significantly rotated counterclockwise after deformation. These results indicate that the supersonic plasma flow retains characteristics of the nonmagnetic limit, while the magnetic field is deformed in response to the supersonic plasma flow. Therefore, the rear-side cylinder structure is largely governed by the supersonic solar-wind plasma flow. This behavior arises from the substantial plasma-pressure enhancement in the

https://doi.org/10.5194/egusphere-2026-3829
Preprint. Discussion started: 25 August 2026

nightside magnetosheath near the Earth, as shown in Fig. 1B. The enhancement occurs because the supersonic solar-wind plasma is compressed between the bow shock and the magnetopause and subsequently diverted around the Earth (day-side magnetosphere). In fact, Spreiter et al. (1966) demonstrated that the near-Earth magnetosheath structure under the supersonic-fluid conditions can be reproduced reasonably well using a hydrodynamic approximation that ignores the magnetic-field effects. On the other hand, enhanced magnetic pressure in the lobe region is required to balance the pressure gradient across the magnetopause. This magnetic-pressure enhancement is produced by magnetic-flux transport from the dayside magnetosphere to the lobe through global magnetic reconnection. This will be discussed in detail in Sect. 5.1.

The magnetic field lines on the rear side of the cylinder in the distant magnetotail gradually bend toward the direction of the IMF. (This feature is evident in the entire picture of the cylinders shown in the center panel of Fig. 3A.) Because the bow shock spreads in a fan shape in the distant magnetotail, the cross-sectional area of the magnetosheath increases. Consequently, the plasma pressure in the magnetosheath decreases. Furthermore, the effect of magnetic-flux transport driven by global magnetic reconnection must also be considered. The simulation results show that the cylinder extends beyond the bow shock into the distant magnetotail. Consequently, in this region, the plasma convection velocity inside the cylinder becomes identical to that outside the cylinder and becomes the solar-wind velocity. Under these conditions, magnetic flux transported into the cylinder by global reconnection cannot be efficiently accumulated on the rear side by convection within the cylinder. As a result, the magnetic pressure at the rear-side boundary of the cylinder is not significantly enhanced. This will be discussed again in Sect. 5.1.

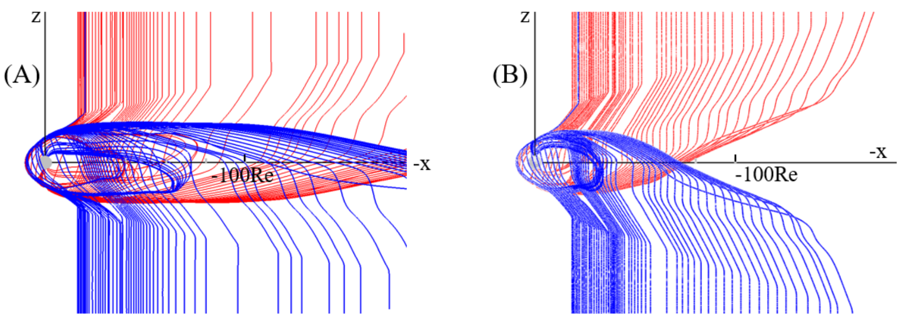

Fig. 3. The red and blue bundles show the magnetic field lines of the cylinder part of Σ_A (the northern hemisphere) and those of Σ_B (the southern hemisphere), respectively, seen from 18 MLT in the equatorial plane for IMF = (0 nT, -4.3 nT, 4.3 nT) and (0 nT, -12.9 nT, 12.9 nT) in panels A and B, respectively. The black dashed lines in both figures represent the bow shock. The magnetic field lines outside the bow shock are the IMF. They appear parallel to the z-axis when viewed from 18 MLT. (The perspective handling in the graphics processing code causes an apparent tilt in the IMF of the cylinder, which should appear parallel to the z-axis.)

https://doi.org/10.5194/egusphere-2026-3829
Preprint. Discussion started: 25 August 2026

To reinforce the conclusion that the predominant magnetic field in the distant magnetotail tends to orient the cylinder closer to the skeletal magnetic field, we investigate the change in the shape of the magnetic field lines on the cylinder when the IMF intensity changes. Figure 3 presents the bundles of the cylinder surfaces with the IMF of (A) (0 nT, -4.3 nT, +4.3 nT) and (B) (0 nT, -12.9 nT, +12.9 nT). (To better understand the cylinder's appearance in the distant magnetotail, the magnetic field lines on the cylinder in the Σ_A and Σ_B surfaces are shown in blue and red, respectively.) Figures 3A and 3B show that the rear side parts of the deformed cylinders for both IMF cases have the same shape closer than about 50 R_E to Earth. In contrast, at locations farther away from Earth, the cylinder appears to be dragged in the IMF direction and does not extend long in the x-axis when the IMF strength increases (Fig. 3B). That is to say, the rear sides of the south and north cylinders (the Σ_A and Σ_B cylinders, respectively) are pulled up and down, respectively, in the z-axis direction. As a result, the bending of the cylinder in the distant magnetotail is caused by the enhanced restoring force of the magnetic field.

The two panels in Fig. 3 exhibit an interesting feature. In the distant magnetotail, the magnetic field lines on the cylinders of Σ_A and Σ_B become progressively twisted: those on Σ_A rotate from the Northern Hemisphere toward the Southern Hemisphere, whereas those on Σ_B rotate in the opposite direction. Consequently, the two cylinders remain adjacent only up to a certain downstream distance, beyond which they diverge. As the IMF strength increases, the restoring force associated with the skeleton magnetic field becomes stronger. Consequently, the twisting of the cylinders is enhanced and the point at which they separate moves closer to the Earth. It is noted that the twisted magnetotail is consistent with the simulation results by Nishida and Ogino (1998).

4.1.2 Dayside Edge Shape of the Magnetosphere as a Manifestation of the Topology Conservation Property

Figure 2D shows that, in contrast to the field lines on the rear side of the cylinder, the front-side field line is not advected downstream by the solar wind but remains connected to the IMF outside the bow shock. This behavior arises from the topology conservation property. This property requires that the two null points maintain almost a fixed position relative to Earth when the solar wind deforms the skeleton magnetic field. Therefore, the magnetic field line connecting fixed null points A and B in the dayside (i.e., the dayside separator) is not blown away toward the antisunward direction by the solar wind. Next, as explained in Sect. 2.2, Fig. 1A shows that, in the two-null, two-separator topology, the subset of γ_A lines extending from null point A to the IMF lies on the Σ_B surface, whereas the subset of γ_B lines extending from null point B to the IMF lies on the Σ_A surface. Consequently, the field line passing through the dayside separator reaches null point B and then continues along the γ_B line lying on the Σ_A surface toward the IMF. Thus, the corresponding field line on the deformed cylinder part of the Σ_A surface is anchored to the γ_B line. Because the null points remain nearly stationary under the solar-wind flow, the field line

https://doi.org/10.5194/egusphere-2026-3829
Preprint. Discussion started: 25 August 2026

connecting null point A to the IMF via the dayside separator and null point B also remains nearly stationary.

It is noted that, in the deformed magnetic field structure, the γ_B line is curved at the magnetosheath, as shown in Fig. 2D. However, in the skeletal magnetic field of Fig. 2B, the γ_B line connected to the null point B is a straight magnetic field line parallel to the z axis, corresponding to the IMF. This curvature is derived from the spatial variation of the plasma convection speed. It is almost zero at the magnetopause, where null point B exists, but gradually increases in the magnetosheath, and it becomes the same as the solar wind flow speed outside the bow shock. This velocity distribution causes the γ_B line (IMF) to curve and approach the separator. As a result, the topology conservation property results in the magnetic field line structure on the dayside edge.

4.1.3 Slit Generation as an Effect of Both the Mechanical Principle and the Topology Conservation Property

On the rear side of the cylinder, the magnetic field is stretched toward the magnetotail by the mechanical principle. In contrast, on the front side, the field lines remain anchored as a consequence of the topology conservation property. The combined action of these two effects deforms the opening of the cylinder, causing it to deviate markedly from its configuration in the skeletal magnetic field. We now examine this deformation in detail.

The shape of the Σ_A cylinder opening of the skeletal field in Figs. 2A and 2B shows approximately circular. The deformed opening shows a crevasse-like structure extending away from the Sun (Figs. 2C and 2D). This crevasse-like structure is called the slit in the present paper. This slit is a narrow window of the lobe open to the solar wind on the flank of the magnetotail. [Stern (1973) called the slit structure a long, narrow “window” and discussed qualitatively the role of this slit structure in the entry of solar wind high-energy particles.] The reason why the slit extends far in the antisunward direction is as follows: The magnetic field lines on the rear side of the deformed cylinder extend in the antisunward direction and tend to bend toward the IMF in the region very far from Earth as shown in Fig. 3A. (The result of this figure is based on the same solar wind parameters as in Figs. 2C and 2D.) In contrast, the magnetic field line of the deformed cylinder on the dayside edge is the γ_B line extending from null point B, which is fixed in the solar wind–magnetosphere region, as noted above.

4.2 Deformation of the Torus

Figures 4A and 4B illustrate the skeletal torus of the Σ_A surface seen from Sun and 18 MLT, respectively. This is the bundle of the skeletal magnetic field lines on the open-closed field boundary (the outermost closed field lines) with the footpoints on the ionosphere in the Southern Hemisphere. Another distinct feature is that these magnetic field lines converge at the null point A in the Northern Hemisphere. In contrast, Figures 4C and 4D show the deformed torus of the Σ_A surface seen from the Sun and 18 MLT,

https://doi.org/10.5194/egusphere-2026-3829
Preprint. Discussion started: 25 August 2026

respectively. These panels show snapshots of the torus magnetic field lines in a quasi-steady state. In each panel, the separator and the γ lines (only the stem lines are shown) are shown in bold red. The black arrows in Figs. 4A and 4C indicate the direction of the IMF. Figure 4A also shows that the tilt of the separator in the skeletal field from the z-axis is about half that of the IMF. The same is true for the separator on the dayside of the deformation field, shown in Fig. 4C.

We can clearly see the deformed Σ_A torus extending toward the night side. This feature is in contrast to the skeletal Σ_A torus, which is symmetrical on the dayside and nightside (Fig. 4B). The size of the skeletal Σ_A torus in the equatorial plane is approximately 20 R_E, whereas the deformed Σ_A torus has a size of about 10 R_E on the dayside (about half of that of the skeletal one) and extends to about 75 R_E on the nightside in the present solar wind condition (Fig. 4D). This long extension of the torus on the night side is consistent with the recent observation by the ARTEMIS satellite of the signature of a closed magnetic field line region in the magnetotail of 60 R_E in the northward IMF condition [Mooney et al., 2024].

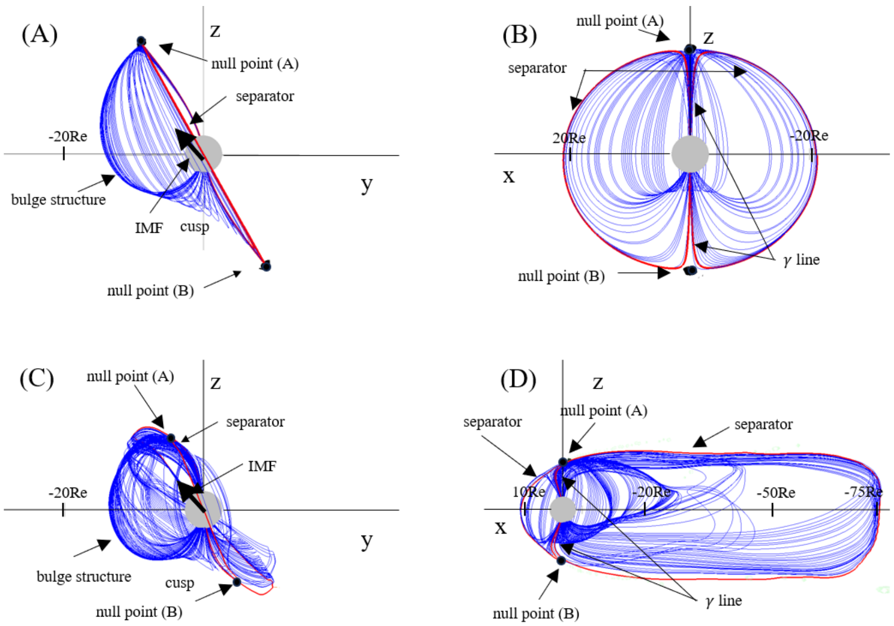

Fig. 4. Blue bundles of numerically calculated magnetic field lines depicting the skeletal torus part of the Σ_A surface with an IMF of (0 nT, -4.3 nT, 4.3 nT) are visualized in two perspectives: panel A as observed from the Sun, and panel B as observed from 18 MLT. The same illustrations of the deformed torus, seen from the Sun and 18 MLT, are shown in panels C and D, respectively. The torus of the Σ_A surface corresponds to the field lines on the open-closed boundary in the ionosphere of the southern hemisphere. Thus, it forms the cusp in the southern hemisphere. The black dots denoted as A and B correspond to null points A and B, respectively. The red bold curves connecting

https://doi.org/10.5194/egusphere-2026-3829
Preprint. Discussion started: 25 August 2026

the two null points are the separator lines. Other red bold curves are part of the γ lines that connect the null point and the ionosphere. The x, y, and z axes point sunward, eastward, and northward, respectively. The black bold arrows in panels A and C indicate the direction of the IMF. The tori in panels A, B, and C are drawn to the same scale, and the torus in panel D is drawn at a reduced scale.

To facilitate understanding of the torus deformation, Figure 5 presents a superposed view of the deformed Σ_A torus (blue) and the deformed Σ_B torus (black), viewed along the IMF direction. The dayside torus exhibits an approximately circular shape with a radius of about 10 R_E. In addition, Figure 5 shows that the orientation of the separator plane on the dayside is not aligned with the IMF direction, because the dayside torus retains approximately the same shape as that of the skeletal field. As shown in Fig. 4C, the tilt angle of the separator plane is approximately half the IMF tilt angle. A similarly inclined separator plane is also observed in the magnetotail within distances of about 30 R_E on the nightside. These results indicate that the influence of the Earth's dipole magnetic field remains significant within approximately 30 R_E in the magnetotail under the present solar-wind conditions. Conversely, the torus gradually loses its thickness in the region outside about 30 R_E and becomes a thin sheet elongated in the IMF direction in the deep magnetotail (especially outside about 50 R_E). Finally, it is recognized that the plane formed by the separator is nearly parallel to the IMF direction in the distant magnetotail up to 75 R_E from Earth.

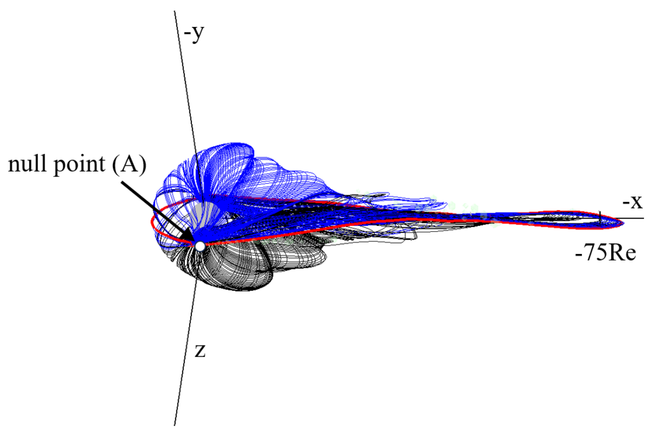

Fig. 5. Bundles of the field lines forming the torus part of the Σ_A surface (blue) and the Σ_B surface (black) combined, seen from the northern hemisphere along the IMF direction. Null point A is shown as a white dot. The red bold curves indicate the separator lines. We notice that the separator on the nightside corresponds to the limit of the torus.

In Sect. 4.1.1, we showed that the rear sides of the skeletal cylinders, which initially extend southward and northward, rotate counterclockwise and clockwise, respectively, when viewed from 18 MLT, thereby

https://doi.org/10.5194/egusphere-2026-3829
Preprint. Discussion started: 25 August 2026

forming the two nightward-extending magnetotail lobes, as illustrated in Fig. 3A. As a result, the antiparallel magnetic field lines of the two cylinders approach each other. Such a magnetic-field configuration would normally lead to the formation of a null point in the magnetotail. However, the topology conservation property requires that the null points in the deformed field remain close to those of the skeletal field in the stationary state. Consequently, the formation of a null point in the magnetotail is prohibited. To satisfy these constraints, closed magnetic field lines are embedded between the two cylinders on the nightside. This configuration also implies that the nightside separator extends far into the magnetotail. In other words, the torus itself extends deep into the magnetotail, as shown in Fig. 2D.

Tanaka et al. (2024) studied the generation mechanism of nightside cell convection in the ionosphere, simulated by REPPU, and discussed the cause of the elongation of plasma sheets based on the behavior of magnetic field line convection in the magnetotail. According to Fig. 7 in Tanaka et al. (2024), the IMF reconnects with open magnetic field lines at the null point in the Southern Hemisphere. These open magnetic field lines are carried into the nightside and reconnect with closed magnetic field lines at the southern null point. At this time, the reconnected closed magnetic field lines are located near the nightside separator and extend far into the nightside. High-pressure plasma is stored in the closed magnetic field line region created in this way, forming a plasma sheet. Therefore, this interpretation builds upon the results of Tanaka et al (2024), and explains why the nightside separator extends far into the magnetotail from the topology conservation property. In our results, the plasma distribution generated by the solar wind colliding with Earth causes the cylinder (open magnetic field line region) to extend parallel to the sun-Earth direction. The restoring force causes the magnetic field lines of these two cylinders to approach the shape of the skeletal magnetic field, causing them to point in opposite directions and separate their tangent surfaces. This creates an elongated torus (a region of closed magnetic field lines). This is the physical process behind the creation of an elongated plasma sheet.

In the extended torus in the nightside, the magnetic field intensity should be weak because this region is sandwiched by two lobes with anti-parallel magnetic fields. From this speculation, the plasma pressure should be enhanced in the extended torus. Thus, the stretched torus on the night side is regarded as the plasma sheet. Other detailed analyses of the torus on the nightside will be treated in future work.

4.3 Topological Distribution in the Magnetotail

In previous sections, we discussed the magnetic field line structure using 3D images of topological boundaries. This time, we will investigate the topological distribution of the two-dimensional (2D) cross-sections in the magnetotail. Here, we will show the distribution of the magnetic field topologies on the noon-meridian plane (zx plane) in Fig. 6A and on the cross-section (yz plane) at x ~ -32 R_E in Fig. 6B. In these panels, the areas of red, green, blue, and black represent the regions of the IMF, open field lines connecting to the northern ionosphere, open field lines connecting to the southern ionosphere, and closed field lines, respectively. The white line in Fig. 6A indicates the cross-section between the noon-meridian

https://doi.org/10.5194/egusphere-2026-3829
Preprint. Discussion started: 25 August 2026

plane and the x ~ -32 R_E plane. In addition, the white line in Fig. 6B depicts the position of the noon-midnight meridian. The one white star in Fig. 6A and the two white stars in Fig. 6B indicate the locations of the intersection of the respective planes with the separator. The four regions of different field line topologies contact each other at these points.

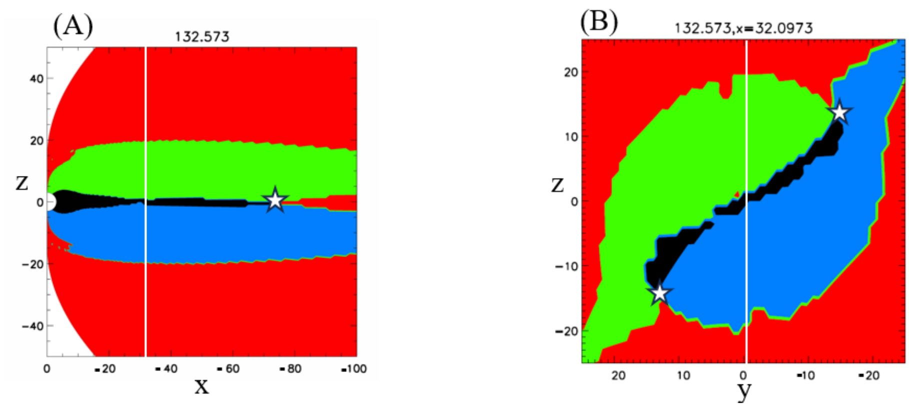

Fig. 6. Panels A and B show the distributions of four categories of magnetic field lines in the midnight meridian plane and the flat plane at x ~ -32 R_E, respectively. Red, green, blue, and black indicate the IMF, open field lines connecting the ionosphere in the Northern Hemisphere, open field lines connecting the ionosphere in the Southern Hemisphere, and closed field lines, respectively. The white stars in the panels indicate the locations of the intersection of the plane with the separator. The white lines in panels A and B indicate the location of x ~ -32 R_E and the midnight meridian, respectively.

Then, we discuss the topologies. Figure 6A confirms that two open magnetic field regions in the noon-midnight meridian, indicated in green and blue, branch toward the north and south, respectively. The limit can be seen from the nightside separator, shown as the red curve of Fig. 2D, which lies at x ~ -75 R_E. In addition, we notice from the distribution of the magnetic topology in the noon-midnight meridian (Fig. 6A) that the thin sheet of the torus (black part) is sandwiched by the two cylinders (green and blue) in the equatorial plane at midnight in the region of x > -75 R_E. Furthermore, the IMF (red part) fills the gap created by the branching of the two cylinders at midnight in the region of x < -75 R_E. The separator passes through the quadruple junction where the four regions of different topology meet, as indicated by the white star in this panel. In addition, from Fig. 6B, the topology distribution in the plane of x ~ -32 R_E (the white line in Fig. 6A) indicates that the two cylinders are close to each other with a thin torus extending almost in the IMF direction. (The distribution of closed magnetic field lines is discussed in more detail below.) This panel shows that the separator passes through the quadruple junctions in the Northern and Southern Hemispheres.

https://doi.org/10.5194/egusphere-2026-3829
Preprint. Discussion started: 25 August 2026

5 Discussions

We have discussed the results obtained through simulations. On the other hand, because it is not easy to reveal the global magnetic field structure through observation, it is difficult to verify magnetic field structures such as the slit structure. One example of the verification is the magnetic field structure of the distant magnetotail. Section 4.1.1 showed that the cylinder bends toward IMF direction in the distant magnetotail because the restoring force of the skeletal field acts to bend the field lines to the IMF. This study employs that the IMF is northward and has a negative By component. Under this condition, as shown in Figs. 2C and 2D, the magnetic field of the Σ_A cylinder extends southwestward in the Southern Hemisphere. On the other hand, in the Northern Hemisphere, the magnetic field of the Σ_B cylinder exhibits a displacement in the opposite direction. As a result, because the two cylinders in the Northern and Southern Hemispheres tilt in opposite directions, a twisted configuration appears as a whole in the distant magnetotail. Such a twisted magnetotail is observed by the GEOTAIL satellite in the northward IMF conditions [Nishida et al., 1995; Maezawa et al., 1997; Maezawa and Hori, 1998; Nishida, 2000].

5.1 Magnetic Pressure in the Lobe that Counteracts the Plasma Pressure of the Magnetosheath

Section 4.1.1 showed that the cylinder and its magnetic field lines in the near-Earth and mid-distance magnetotail are stretched in the antisunward direction by the solar wind plasma flow. This result is due to the dominant influence of the solar wind pressure, which strongly distorts the magnetic field. To maintain force balance against this plasma pressure, the magnetic pressure must be enhanced. It should be noted that the restoring force associated with the skeletal magnetic field cannot support the magnetosheath plasma pressure, because it acts in the same direction as the pressure-gradient force. On the other hand, global magnetic reconnection transports magnetic flux from the solar wind to the magnetosphere. Thus, the magnetic flux transported by convection to the lobe region is capable of providing the plasma pressure in the magnetosheath. We investigate how magnetic flux transported into the lobe region contributes to balancing the magnetosheath plasma pressure, based on the simulation results.

The mechanical principle is expressed as a balance between the plasma forces (the pressure-gradient force ($\nabla_\perp p$) and the inertia force ($\rho(\boldsymbol{v} \cdot \nabla)\boldsymbol{v}_\perp$)) and the Lorentz force ($\boldsymbol{J}_\perp \times \boldsymbol{B}$). The inertia term can be neglected because the plasma flow is nearly straight in the magnetosheath in near-Earth and mid-distance magnetotail. Furthermore, the simulation results indicate that the magnetic field is weakly curved on the rear side of the cylinder. Under these conditions, Equation (10) reduces to the following expression of the force balance:

$$\nabla_\perp p \simeq \boldsymbol{J}_\perp \times \boldsymbol{B} \simeq -\frac{\nabla|\boldsymbol{B}|^2}{2\mu_0}.$$

As noted above, the plasma-pressure distribution retains characteristics of the nonmagnetic limit. Consequently, enhanced magnetic pressure is required on the rear side of the cylinder to maintain force balance. Here, we show, using the simulation results, that this magnetic-pressure enhancement is produced by magnetic flux transported from the IMF into the magnetosphere through global magnetic reconnection. Because magnetic field lines are convected with the plasma flow, we select a representative

https://doi.org/10.5194/egusphere-2026-3829
Preprint. Discussion started: 25 August 2026

convection streamline originating outside the magnetosphere and examine the evolution of magnetic field lines along this streamline. The result is shown in Fig. 7A. In Fig. 7A, Point 1 is defined on a representative convection streamline in the solar wind, and ten additional points are assigned along the streamline downstream from this location. The streamline crosses the cylinder surface between Points 3 and 4 and subsequently follows a trajectory that circulates around the open-field-line region inside the cylinder. To investigate the transport of magnetic flux, Figure 7B shows the magnetic field lines passing through each of the points defined in Fig. 7A. When the convection streamline crosses the cylinder surface between Points 3 and 4, the magnetic topology changes. As shown in Fig. 7C, the field line passing through Point 3 (hereafter, field line #3) is connected to the IMF at both ends, whereas the field line passing through Point 4 (field line #4) is an open field line connected to the northern ionosphere. Therefore, the topological transition between #3 and #4 occurs through field-line bifurcation at null point A. (The global magnetic reconnection process and the associated bifurcation between IMF and magnetospheric field lines will be discussed in detail in a separate paper.) In Fig. 7B, the color of each field line represents the perpendicular convection velocity, $\boldsymbol{v}_\perp$. Newly reconnected open field lines in the dayside magnetosphere are predominantly green, indicating relatively rapid convection. As these field lines are transported into the nightside lobe, their color gradually changes to purple, indicating a reduction in $\boldsymbol{v}_\perp$. From the magnetic induction equation, we obtain

$$\frac{\partial|\mathbf{B}|}{\partial t}+(\boldsymbol{v}_\perp\cdot\nabla)|\mathbf{B}|=\frac{D|\mathbf{B}|}{Dt}=-|\mathbf{B}|(\nabla\cdot\boldsymbol{v}_\perp)-|\mathbf{B}|\boldsymbol{v}_\perp(\hat{e}\cdot\nabla)\hat{e}. \quad (11)$$

Since the magnetic field lines in the nightside lobe are nearly straight in Fig. 7B, the curvature term (the second term of r.h.s.) in Eq. (11) is small. Thus, since the observed deceleration of the convection flow implies $\nabla\cdot\boldsymbol{v}_\perp<0$, this result leads to an increase in $|\mathbf{B}|$. Hence, magnetic flux is accumulated in the nightside lobe. The resulting enhancement of magnetic pressure is consistent with the force balance required to support the magnetosheath pressure gradient.

Because open field lines shown in Fig. 7B are connected to the ionosphere, their transport into the lobe is influenced by ionospheric coupling. However, the simulation results shown in Fig. 7 were obtained with ionospheric effects included. These results suggest that the magnetic-flux accumulation in the lobe is a robust feature of the global convection system and is not critically dependent on ionospheric coupling.

https://doi.org/10.5194/egusphere-2026-3829
Preprint. Discussion started: 25 August 2026

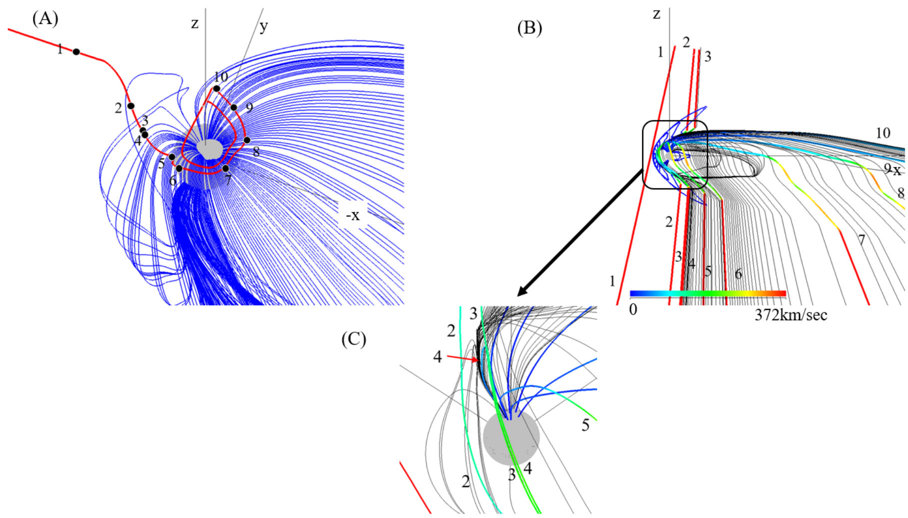

Fig. 7. (A) The red line represents the streamline of plasma convection flowing from the solar wind (point 1) to the magnetosphere (point 10), as viewed from above the northern hemisphere on the dusk side. 10 points are selected on the streamline. The convection streamline crosses the cylinder surface between No. 3 and No. 4 and circulate within the cylinder. The bundle of blue curves denotes the cylinder part of the Σ_A surface. (B) Overall view of magnetic field lines originating from the 10 selected points along the convection streamline of panel A. Field lines are color-coded by the perpendicular velocity magnitude $|v_\perp|$. The blue contours indicate the plasma pressure distribution with a contour interval of 0.2 nPa in the noon-midnight meridian. The bundle of gray curves denotes the cylinder part of the Σ_A surface. The IMF of #3 suddenly changes to the open field line of #4 because the convection streamline passes through the cylinder surface. (C) Enlarged view of the region outlined by the rectangle in Panel B, viewed from above the Northern Hemisphere.

Finally, to demonstrate that the restoring force associated with the skeletal magnetic field remains effective in the distant magnetotail, we explain why magnetic-field convection does not lead to significant magnetic-flux accumulation in this region. Figure 7B shows that the convection speed on the front side approaches the solar-wind speed in the region beyond the bow shock. This result indicates that the magnetic field within the cylinder (the open field lines) gradually approaches the surrounding IMF in the distant magnetotail. A similar feature is expected on the rear side, although the distance at which the open field lines approach the IMF is much greater than on the front side. As a result, in regions far from the Earth, the solar wind crosses the boundary of the cylinder with little dynamical modification. Therefore, magnetic-flux accumulation in the cylinder does not occur in the region far from the Earth.

https://doi.org/10.5194/egusphere-2026-3829
Preprint. Discussion started: 25 August 2026

5.2 The Possible Reasons Why Magnetic Topology is Conserved

In Sect. 4, we discussed that under obliquely northward IMF conditions, the topology of the vacuum magnetic field (the skeletal magnetic field) is conserved even when the magnetic field is deformed by the solar wind based on the simulation results. This means that when considering the physical processes of the solar wind–magnetosphere system as an interaction between the magnetic field and plasma, the plasma dynamics deforms the magnetic field within a constraint of the magnetic topology conservation. In other words, the topology controls the mechanical interaction between the magnetic field and plasma dynamics. So, it is important to consider why the magnetic topology is conserved.

While a rigorous quantitative evaluation of this point is not easy, it can be understood through the following three physical factors. Firstly, the vacuum magnetic field that provides the basic topology corresponds to the minimum state of magnetic field energy and serves as a "ground state" for the system. Therefore, even if the magnetic field is deformed by an external force, a restorative response appears to act on the magnetic field and attempts to return it to its original vacuum magnetic field structure. Secondly, the Earth's magnetic field is sufficiently strong to suppress the intrusion of solar wind plasma in the magnetopause. Therefore, magnetic field deformation caused by the solar wind does not significantly alter the overall magnetic field topology. Thirdly, the skeletal magnetic field has the magnetic field structure ready for global magnetic reconnection between IMF and Earth's magnetic field. This fact means that the magnetic field structure does not need to change so significantly when the reconnection in deed occur in the plasma environment. For these reasons, under obliquely northward IMF conditions, the magnetic field topology is considered to be conserved.

In this study, we assumed that the topology of the skeletal magnetic field remains unchanged (the topology conservation property) even when deformed by solar wind plasma. However, this assumption does not always hold in the real solar wind−magnetosphere system. It should be noted that Park et al. (2015) showed by a simulation that, exceptionally, small-scale substorm-like disturbances can occur even under northward IMF conditions. In these cases, reconnection is reported to occur on the nightside. Therefore, the two-null, two-separator structure exceptionally collapses under northward IMF conditions. The present study excludes such exceptional circumstances. This topic may be an interesting future work as an application of the present theory based on the mechanical principle and the topology conservation property.

6 Conclusion

The main results are summarized as follows.

1. The magnetic-field structure of the solar wind–magnetosphere system under the obliquely northward IMF condition evolves from the vacuum magnetic-field configuration (the superposition of the Earth's main magnetic field and a uniform IMF) by the force balance (the mechanical principle) subject to the constraint that the topology of the original vacuum magnetic field is

https://doi.org/10.5194/egusphere-2026-3829
Preprint. Discussion started: 25 August 2026

conserved (the topology conservation property). The vacuum magnetic field can be called the skeletal field.

2. In the near-Earth and mid-tail regions of the magnetotail, the magnetic field lines of the rear-side cylinder extend in the antisunward direction under the influence of the tailward solar-wind flow, whereas they bend toward the IMF direction in the distant magnetotail under the influence of a restoring force that acts to return the field toward the skeletal-field configuration. Consequently, the two cylinders twist in different directions in the distant magnetotail. On the other hand, the null points are not transported to the nightside by the solar wind. Therefore, the magnetic field lines connected to the separator on the dayside of the cylinder become the field lines defining the dayside edge of the cylinder. As a result, the opening of the cylinder deforms into a long, narrow slit extending along the flank of the magnetotail.
3. The nightside separator is stretched in the antisunward direction by the deformation of the two cylinders. This deformation also stretches the torus (the closed field line region) and forms the plasma sheet.

The purpose of this paper is to clarify the fundamental physical processes underlying the interaction between magnetic topology and plasma dynamical processes in the solar wind–magnetosphere system. Therefore, we have only discussed how this interaction gives rise to the basic magnetic field structures of the magnetotail and plasma sheet. The plasma distribution, convection, bulk flow patterns, and current systems formed by this interaction will be discussed in detail in future work.

Code and data availability

The simulation results employed for this study and the sample code which read the results are available at http://polaris.nipr.ac.jp/~sfujita/exchange/skeleton1/.

For the analysis, we used a commercially available drawing software called Clef3D MFC (https://icfd.co.jp/en/product/visualize.html).

Author contributions

SF conducted the numerical simulation and analyzed the simulation results. SF, MW, TT, and DSC wrote the paper.

Competing interests

No competing interests

Disclaimer

Copernicus Publications remains neutral with regard to jurisdictional claims made in the text, published maps, institutional affiliations, or any other geographical representation in this paper. While Copernicus

https://doi.org/10.5194/egusphere-2026-3829
Preprint. Discussion started: 25 August 2026

Publications makes every effort to include appropriate place names, the final responsibility lies with the authors. Views expressed in the text are those of the authors and do not necessarily reflect the views of the publisher.

Acknowledgements

SF gratefully acknowledges valuable discussions with K.-H. Glassmeier of the Technical University of Braunschweig. The simulation was performed with the computers installed at the Center for Engineering and Technical Support of the Institute of Mathematical Statistics and the Polar Science Computer System at the National Institute of Polar Research. The authors used ChatGPT for proofreading some of the manuscripts.

Financial support

This research was supported by a “Challenging Exploratory Research Projects for the Future" grant titled “Infrastructure Development for the Global Reanalysis Data of the Magnetosphere-Ionosphere System” from the Research Organization of Information and Systems. The research was also supported by the Japan Society for the Promotion of Science (JSPS KAKENHI Grants JP20K03894, JP24K06989, and JP24H00277).

References

Cowley, S. W. H. (1973), A qualitative study of the reconnection between the Earth's magnetic field and an interplanetary field of arbitrary orientation, Radio Sci., 8(11), 903-913, doi:10.1029/RS008i011p00903.

Craig, I. J. D., R. B. Fabling and P. G. Watson, The Power Output of Spine and Fan Magnetic Reconnection Solutions, The Astrophysical Journal, 485 1, 383, 1997, https://dx.doi.org/10.1086/304411

Crooker, N. U. (1979), Dayside Merging and Cusp Geometry, J. Geophys. Res., 84(A3), 951-959.

Crooker, N. U., J. G. Lyon, and J. A. Fedder (1998), MHD model merging with IMF By: Lobe cells, sunward polar cap convection, and overdraped lobes. J. Geophys. Res., 103(A5), 9143-9151, doi: 10.1029/97JA03393.

Dorelli, J. C., A. Bhattacharjee, and J. Raeder (2007), Separator reconnection at Earth's dayside magnetopause under generic northward interplanetary magnetic field conditions, J. Geophys. Res., 112, A02202, doi:10.1029/2006JA011877.

Dungey, J. W., Interplanetary magnetic field and the auroral zones, Phys. Rev. Lett., 6, 47-49, 1961, doi:10.1103/PhysRevLett.6.47.

Dungey, J. W., Interplanetary magnetic field and the auroral zones, AFCRL-62-423, 1962.

Greene, J. M. (1988), Geometrical Properties of Three-Dimensional Reconnecting Magnetic Fields with Nulls, J. Geophys. Res., 93(A8), 8583-8590, doi:10.1029/JA093iA08p08583.

Haynes, A. L., and C. E. Parnell, A trilinear method for finding null points in a three-dimensional vector space, Phys. Plasmas, 14, 082107 (2007); doi:10.1063/1.2756751.

https://doi.org/10.5194/egusphere-2026-3829
Preprint. Discussion started: 25 August 2026

Hesse, M., and K. Schindler (1988), A theoretical foundation of general magnetic reconnection, J. Geophys. Res., 93(A6), 5559-5567, doi:10.1029/JA093iA06p05559.

Hones, E. W., Craven, J. D., Frank, L. A., Evans, D. S., and Newell, P. T. (1989). The horse-collar aurora: A frequent pattern of the aurora in quiet times. Geophysical Research Letters, 16(1), 37-40. https://doi.org/10.1029/GL016i001p00037

Hughes, W. J., The magnetopause, magnetotail, and magnetic reconnection, in *Introduction to Space Physics*, pp. 227-287, 1995, ed. by M. G. Kivelson and C. T. Russell, Cambridge Univ. Press.

Lau, Y.-T. and Finn, J. M. (1990), Three-dimensional kinematic reconnection in the presence of field nulls and closed field lines, *Astrophysical Journal*, 350, 672-691.

Li Ting, Priest Eric, and Guo Ruilong (2021), Three-dimensional magnetic reconnection in astrophysical plasmas, Proc. R. Soc. A.47720200949, http://doi.org/10.1098/rspa.2020.0949

Lundin, R., and S. Barabash, The wakes and magnetotails of Mars and Venus, Advances in Space Research 33, 11, 2004, 1945-1955, https://doi.org/10.1016/j.asr.2003.07.054.

Maezawa, K., T. Hori, T. Mukai, Y. Saito, T. Yamamoto, S. Kokubun, A. Nishida,
Structure of the distant magnetotail and its dependence on the IMF By component: GEOTAIL observations, Advances in Space Research, 20, 4-5, 1997, 949-959, https://doi.org/10.1016/S0273-1177(97)00503-6.

Maezawa, K., and Hori, T. (1998). The distant magnetotail: Its structure, IMF dependence, and thermal properties. In New Perspectives on the Earth's Magnetotail (eds A. Nishida, D.N. Baker and S.W.H. Cowley). 105, 1-19.

Mooney, M. K., Milan, S. E., and Bower, G. E. (2024). Plasma observations in the distant magnetotail during intervals of northward IMF. Journal of Geophysical Research: Space Physics, 129, e2023JA031999. https://doi.org/10.1029/2023JA031999

Morfill, G., and Scholer, M. (1972), Reconnection of the geomagnetic tail deduced from solar-particle observations, J. Geophys. Res., 77(22), 4021-4024Doi:10.1029/JA077i022p04021.

Moriguchi, T., A. Nakamizo, T. Tanaka, T. Obara, and H. Shimazu (2008), Current systems in the Jovian magnetosphere, J. Geophys. Res., 113, A05204, doi:10.1029/2007JA012751.

Nishida, A., and K. Maezawa (1971), Two basic modes of interaction between the solar wind and the magnetosphere, J. Geophys. Res., 76(10), 2254-2264, doi:10.1029/JA076i010p02254.

Nishida, A., *Geomagnetic Diagnosis of The Magnetosphere*, Springer-Verlag, New York, 1978.

Nishida, A., T. Mukai, T. Yamamoto, Y. Saito, S. Kokubun, and K. Maezawa (1995), GEOTAIL observation of magnetospheric convection in the distant tail at 200 RE in quiet times, J. Geophys. Res., 100(A12), 23663-23675, doi:10.1029/95JA02519.

Nishida, A. and Ogino, T. (1998). Convection and Reconnection in the Earth's Magnetotail. In New Perspectives on the Earth's Magnetotail (eds A. Nishida, D.N. Baker and S.W.H. Cowley). 105, 507-577. https://doi.org/10.1029/GM105p0061

Nishida, A. The Earth's Dynamic Magnetotail. Space Science Reviews, 91, 507-577 (2000). https://doi.org/10.1023/A:1005223124330

https://doi.org/10.5194/egusphere-2026-3829
Preprint. Discussion started: 25 August 2026

Park, K. S., D.-Y. Lee, T. Ogino, and D. H. Lee (2015), MHD simulations using average solar wind conditions for substorms observed under northward IMF conditions, J. Geophys. Res. Space Physics, 120, 7672-7686, doi:10.1002/2015JA021005.

Priest, E. and T. Forbes, Reconnection in Three Dimensions, in *Magnetic reconnection*, pp. 230-289, 2000, Cambridge University Press.

Raeder, J., J. Berchem, and M. Ashour-Abdalla (1998), The Geospace Environment Modeling Grand Challenge: Results from a Global Geospace Circulation Model, J. Geophys. Res., 103 (A7), 14,787-14,797.

Russell, C. T., J. G. Luhmann, and R. J. Strangeway, Solar-wind interaction with magnetized obstacles, in *Space Physics, An Introduction*, pp. 222-247, Cambridge University Press, Cambridge, 2016

Schindler, K., M. Hesse, and J. Birn (1988), General magnetic reconnection, parallel electric fields, and helicity, J. Geophys. Res., 93(A6), 5547-5557, doi: 10.1029/JA093iA06p05547.

Siscoe, G. L., The Magnetospheric boundary, in Physics of Space Plasmas, edited by T. Chang, G. B. Crew, and J. R. Jasperse, pp. 3-78, Cambridge, Mass., 1988.

Siscoe, G. L., N. U. Crooker, G. M. Erickson, B. U. Sonnerup, K. D. Siebert, D. R. Weimer, W. W. White, and N. C. Maynard (2000), Global geometry of magnetospheric currents inferred from MHD simulations, in Magnetospheric Current Systems, Geophys. Monogr. Ser., vol. 118, edited by S. Ohtani et al., pp. 41-52, AGU, Washington, D. C., doi:10.1029/GM118p0041.

Siscoe, G. L., G. M. Erickson, B. U. O. Sonnerup, N. C. Maynard, K. D. Siebert, D. R. Weimer, and W. W. White (2001), Global role of $E_{||}$ in magnetopause reconnection: An explicit demonstration, J. Geophys. Res., 106(A7), 13,015-13,022, doi:10.1029/2000JA000062.

Sonnerup, B. U. (1974), Magnetopause reconnection rate, J. Geophys. Res., 79(10), 1546-1549, doi:10.1029/JA079i010p01546.

Spreiter, J. R., A. L. Summers, and A. Y. Alksne, Hydromagnetic flow around the magnetosphere, Planet. Space Sci., 14, 223-253, 1966. https://doi.org/10.1016/0032-0633(66)90124-3

Stern, D. P. (1973), A study of the electric field in an open magnetospheric model, J. Geophys. Res., 78(31), 7292-7305, doi:10.1029/JA078i031p07292.

Tanaka, T. (1999), Configuration of the magnetosphere-ionosphere convection system under northward IMF conditions with nonzero IMF By, J. Geophys. Res}, 104(A7), 14683-14690, doi:10.1029/1999JA900077.

Tanaka, T. (2007), Magnetosphere-Ionosphere Convection as a Compound System, Space Sci Rev, 133, 1-72, DOI 10.1007/s11214-007-9168-4.

Tanaka, T., A. Nakamizo, A. Yoshikawa, S. Fujita, H. Shinagawa, H. Shimazu, T. Kikuchi, and K. K. Hashimoto (2010), Substorm convection and current system deduced from the global simulation, J. Geophys. Res., 115, A05220, doi:10.1029/2009JA014676.

Tanaka, T. (2015), Substorm Auroral Dynamics Reproduced by Advanced Global Magnetosphere-Ionosphere (M-I) Coupling Simulation, in Auroral Dynamics and Space Weather (eds Y. Zhang and L. J. Paxton), John Wiley & Sons, Inc., Hoboken, NJ. doi: 10.1002/9781118978719.ch13

https://doi.org/10.5194/egusphere-2026-3829
Preprint. Discussion started: 25 August 2026

Tanaka, T., T. Obara, M. Watanabe, S. Fujita, Y. Ebihara, and R. Kataoka (2017), Formation of the Sun-aligned arc region and the void (polar slot) under the null-separator structure, J. Geophys. Res., Space Physics, 122, doi:10.1002/2016JA023584.

Tanaka, T., Obara, T., Watanabe, M., Fujita, S., Ebihara, Y., Kataoka, R., and Den, M. (2018). Cooperative roles of dynamics and topology in generating the magnetosphere-ionosphere disturbances: Case of the theta aurora. Journal of Geophysical Research: Space Physics, 123, 9991-10,008. https://doi.org/10.1029/2018JA025514

Tanaka, T., Obara, T., Watanabe, M., Fujita, S., Ebihara, Y., Kataoka, R., and Den, M. (2019). Magnetosphere-ionosphere convection under the due northward IMF. Journal of Geophysical Research: Space Physics, 124, 6812-6832. https://doi.org/10.1029/2019JA026547

T. Tanaka, Y. Ebihara, M. Watanabe, S. Fujita, and R. Kataoka (2024), Multiple convection cells induced by in-front and off-front interactions between the obliquely northward IMF and the geomagnetic field, Journal of Geophysical Research: Space Physics, 129, e2023JA031994. https://doi.org/10.1029/2023JA031994

Wang, X., and A. Bhattacharjee (1996), A three-dimensional reconnection model of the magnetosphere: Geometry and kinematics, J. Geophys. Res., 101(A2), 2641-2653, doi:10.1029/95JA02184.

Watanabe, M., K. Kabin, G. J. Sofko, R. Rankin, T. I. Gombosi, A. J. Ridley, and C. R. Clauer (2005), Internal reconnection for northward interplanetary magnetic field, J. Geophys. Res., 110, A06210, doi:10.1029/2004JA010832.

Watanabe, M., G. J. Sofko, K. Kabin, R. Rankin, A. J. Ridley, C. R. Clauer, and T. I. Gombosi (2007), Origin of the interhemispheric potential mismatch of merging cells for interplanetary magnetic field By-dominated periods, J. Geophys. Res., 112, A10205, doi:10.1029/2006JA012179.

Watanabe, M., K. Kabin, G. J. Sofko, R. Rankin, T. I. Gombosi, and A. J. Ridley (2010), Dipole tilt effects on the magnetosphere-ionosphere convection system during interplanetary magnetic field By-dominated periods: MHD modeling, J. Geophys. Res., 115, A07218, doi:10.1029/2009JA014910.

Xiong, P., Fujita, S., Watanabe, M., Tanaka, T., and Cai, D. (2024), Identifying and Visualizing Terrestrial Magnetospheric Topology using Geodesic Level Set Method. Computer Graphics Forum, 43: e14994. https://doi.org/10.1111/cgf.14994